Molecular *in silico* docking interventions in various SARS-CoV-2 receptor targets involving bioactive herbal compounds of *Andrographis paniculata* (Burm. f.) Nees against COVID-19

Manubotula Durga Sahithya, Mote Srinath, Bukhya Chaitanya Kumar* and Charu Chandra Giri♦

Centre for Plant Molecular Biology, Osmania University, Hyderabad-500007, Telangana State, India
*Department of Genetics, Osmania University, Hyderabad-500007, Telangana State, India

Article Info

Abstract

Andrographis paniculata Burm.f. Nees is a medicinal plant of huge pharmaceutical value, having antiviral, anti-inflammatory properties and it was also referred to as a wonder drug in the Spanish Flu pandemic during 1918 for arresting the viral growth or spread. Due to the lack of proper available vaccine and side effects of the drugs, we need an effective alternative strategy for the COVID-19 treatment and management. Bioactive secondary metabolites from this plant were docked to various targets of SARS-CoV-2 and the binding energies were compared with two reference drugs, nelfinavir and hydroxychloroquine. *In silico* pharmacophysical properties and toxicity predictions revealed out of 17 compounds from *A. paniculata*, 9 compounds, namely; andrographolide, andrographic acid, neoandrographolide, 14-deoxyandrographolide, 14-deoxy 11, 12-didehydroandrogra-pholide, onysilin, 14-deoxy 14, 15-dehydroandrographolide, 3, 4-dicaffeoylquinic acid and isoandrographolide have shown higher inhibition at multiple targets. Further, they have shown superior permeability, bioavailability properties and low levels of toxicity. Hence, the bioactive compounds from *A. paniculata* could be effective candidates for drug designing and could be the choice of traditional therapeutic option against COVID-19. Use of *A. paniculata* active constituents for the patients in the initial stages of infection may prevent its transition into severe symptoms.

1. Introduction

At the end of the year 2019, a new type of pneumonia with unknown cause was detected in Wuhan, China with common symptoms which includes fever, fatigue, dry cough, diarrhea, and difficulty in breathing (Lu *et al*., 2020). The causative agent was identified as a virus and named as SARS-CoV-2. The disease was named coronavirus disease 2019 (COVID-19) by WHO on 11 February 2020. About 169,597,415 confirmed COVID-19 cases with over 3,530,582 deaths were reported globally at the time of writing this manuscript. The United States of America has the most confirmed cases (32,916,501) around the world. India has recorded nearly 28 million COVID-19 cases - second only to the US and 325,972 deaths-third only after the US and Germany to record more than 30000 deaths. Globally, one in every three new cases were reported from India (The world health organization information bulletin). It is the new epicenter of the global pandemic.The next among the top hit countries are Brazil (16,391,930), and the France (5,557,692) according to WHO (https://covid19.who.int/). According to the report from the Ministry of Health and Family Welfare, India, at the start of the second wave in the April 2021, India confirmed 11,000 cases per day, but in the next 50-60 days, the number of cases rose to 90000 daily average. Now, India has been consistently reporting more than 150,000 cases per day. 4.14 lakh cases in one day, the biggest daily spike in

the second wave. According to the worldwide reporting a 300% increase in COVID-19 active cases in India alarms the severity of the second wave with 4000 deaths daily, at least 153 people dying every hour. The positivity rate was increased from 12% to 20% in India. The presence of coronavirus variants causing higher disease transmission in the second wave than the first wave. According to US Centers for disease control and prevention (CDC), the UK variant has 50% higher transmission rate. The L452R mutation that was found in the B1.671 Indian variant has also shown similar disease transmission rate as the UK variant even in the people who are staying in the indoors. Even the vaccines did not stop the spread of the disease transmission and can only reduce the disease severity and helps in early recovery. According to the data released by the Indian Government, 2-4 persons per 10000 got positive after vaccination.

SARS-CoV-2 belongs to β-coronavirus family with single-stranded RNA as genetic material and it has shown high similarity with other coronaviruses and SARS (Lu *et al*., 2020; Lu *et al*, 2020). The primary symptoms of the COVID-19 are fever, cough, difficulty in breathing, similar to SARS and MERS (Chen *et al*., 2020). While conventional methods of drug discovery could take years, the *in silico* immuno-informatics and docking approaches to search for possible active biomolecules for the SARS-CoV-2 might speed up the process as a supplement. The bioactive compounds may target most variable proteins, *i.e*., structural and non-structural proteins (NSP) of the SARS-CoV-2. The structural proteins include the spike glycoprotein (SGpro), nucleocapsid protein (Npro), membrane glycoprotein (MGpro), and an envelope protein (Epro) whereas non-structural proteins consists of papain-like protease (PLpro), chymotrypsin-

Corresponding author: Dr. Charu Chandra Giri
Former Director, Centre for Plant Molecular Biology, Osmania University, Hyderabad-500007, Telangana State, India
E-mail: giriccin@yahoo.co.in
Tel.: +91-9949493532

like protease (3CLpro/Nsp5), RNA binding protein (Nsp9), uridylate-specific endoribonuclease (Nsp15) and RNA-directed RNA polymerase (Pol/RdRp/Nsp12) (Mousavizadeh and Ghasemi. 2021). The diagrammatic representation of target proteins is shown in the (Figure 1a and 1b). The SGpro helps to attach a host cell membrane and enters into the cell through a receptor-mediated interaction (Wu *et al.* 2020). The Npro is involved in the formation of helical nucleocapsid of virion (Cascarina and Ross. 2020). The MGpro control the major functions of the virus. It acts as a multipass trans-membrane protein and forms a major part of the envelope which contributes to the shape of the virion (Hsieh *et al.*, 2008). The Epro is an integral membrane protein that plays a critical role in pathogenesis, formation of an envelope, assembly, budding, and releases (O'Donnell *et al.*, 2020). The PLpro and 3CLPro are necessary for virus survival in the host cell. They both cleave polyprotein 1 a/b (PPa/b) encoded by SARS-CoV-2 and yield proteins involved in various functions such as infection, transcription, and replication (Goswami *et al.*, 2020). PLpro is believed to be involved in blocking the host's innate immune response (Balasubramaniam and Reis, 2020), whereas RdRp plays an important role in RNA replication (Venkataraman *et al.*, 2018; Stubbs and TeVelthuis, 2014). All these proteins are essential for the transmission and virulence of the virus. The severity of the infection could be reduced by inhibiting the action of any of these target proteins.

Our efforts are aimed to target multiple proteins and inhibit those using natural substrates by *in silico* approach. Because, the off label drugs used in the treatment of COVID-19 have shown a significant degree of toxicity and severe side effects (Gevers *et al.*, 2020; García *et al.*, 2020). The drug repurposing studies indicated that nelfinavir (NFR) was identified as a potential inhibitor of Spro, Nsp9, Nsp15, and RdRp targets (Barros *et al.*, 2020; Tallei *et al.*, 2020; Xu *et al.*, 2020). As well, hydroxychloroquine (HCQ), an antimalarial drug considered as effective in the current treatment of severe infection (Colson *et al.*, 2020; Mitjà and Clotet, 2020; Wang *et al.*, 2020). But, practicing traditional Indian medicine has many advantages over currently used medicines with its easy availability, cost effective and low or meager side effects. The natural plant-based compounds were used in the previous two pandemics, *e.g.*, SARS-CoV and MERS-CoV. This has proved that these compounds have tremendous potentials against viral diseases (Li *et al.*, 2005). Therefore, in the present work, we have selected *Andrographis paniculata* (*A. paniculata*), a well-known medicinal plant used as a folklore remedy to treat many infectious diseases in India and other Southeast Asian countries (Dai *et al.*, 2019). During the 1919 pandemic due to the influenza virus, *A. paniculata* was used effectively to suppress the contamination and credited as a wonder drug. The plant decoction was used for disease management and to restrict the spread of infection (Hancke *et al.*, 1995). The plant is referred to as the next big immune booster because of its various medicinal properties and the presence of active principles. It has shown immune-boosting (Churiyah *et al.*, 2015), antioxidant (Polash *et al.*, 2017; Mussard *et al.*, 2019; Puri *et al.*, 2019), anti-inflammatory (Yen *et al.*, 2018; Weng *et al.*, 2018) and antiviral (Angamuthu *et al.*, 2019; Li *et al.*, 2020; Paemanee *et al.*, 2019; Ali-Seyed and Vijayaraghavan, 2020) properties. There was also some evidence of treating the patients with andrographis (Kan Jang, Swedish Herbal Institute) prove better results than amantadine drugs which are approved by the FDA in the treatment of Asian flu and influenza A (https://www.rxlist.com/andrographis/supple ments.htm). Further, the uncertainty over the launch of vaccine candidates in the near future and the availability of effective antiviral drugs, it becomes urgent to look for alternatives. Hence, *A. paniculata* finds its significance and could be a candidate for evaluation in the SARS-CoV-2 disease treatment and/or management.
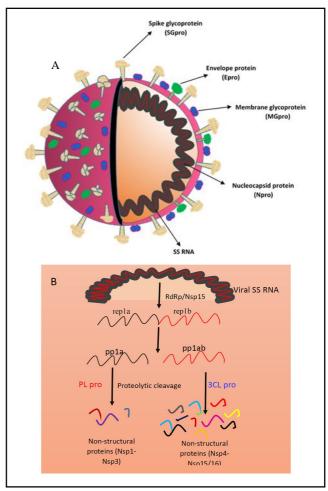

Figure 1: Schematic representation of cross section of SARS-CoV-2 virus. (a) Different structural proteins of SARS-CoV-2 virus and single stranded genomic RNA enveloped with nucleo-capsid protein. (b) The SARS-CoV-2 genome containing two open reading frames (ORF1 and ORF2) which encode two large overlapping polyproteins, pp1a (~450 kDa) and pp1ab (~750 kDa), from which the non-structural proteins are produced by an extensive proteolytic action of 3CLpro and PLproRdRp-RNA dependent RNA polymerase; ORF-open reading frame; pp1a and pp1ab-polyprotein 1a and polyprotein 1ab; Nsp-Non-structural proteins; PLpro-Papain-like protease; 3CL pro-3 Chymotrypsin-like protease.

In the present study, investigation was carried out involving known bioactive compounds from *A. paniculata* against several target proteins of SARS-CoV-2 at their catalytic sites. Exploration of the effective compounds with high, inhibiting properties, finds its importance in clinical infection management. The results were compared with binding energies of both HCQ and NFR. Further, our results will provide valuable information elucidating the role of *A. paniculata* bioactive molecules in COVID-19 disease treatment and management.
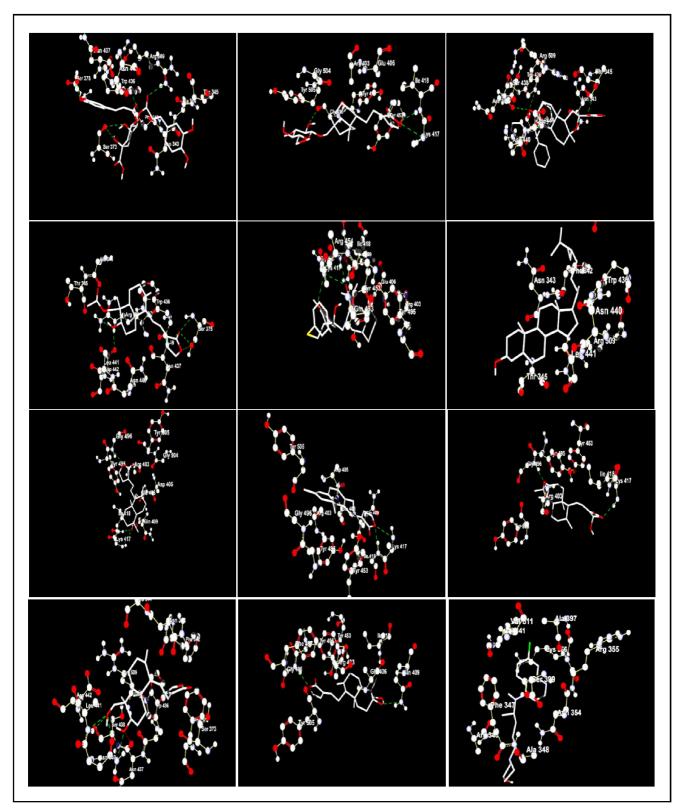
Figure 2: Docking conformers of active molecules present in *A. paniculata* at SGpro (6VSB) receptor. (a) 3,4-dicaffeoylquinic acid, (b) neoandrographolide, (c) isoandragrapholide, (d) 19-o-acetyl-14-deoxy 11,12-didehydroandrographolide, (e) nelfinavir, (f) beta-sitosterol, (g) andrograpanin, (h) andrographolactone, (i) 3,19-isopropylidene andrographolide, (j) 14-deoxyandrographolide, (k) andrographolide, (l) hydroxychloroquine.

2. Material and Methods

2.1 Identification of potential targets, structure prediction, homology modeling and validation

In the present study, seven potential targets of SARS-CoV-2 were identified. 3D structural models of SGpro (PDB ID-6VSB), Npro (6YI3), 3CLpro (6LU7), PLpro (6W9C), Nsp9 (6W4B), Nsp15 (6VWW), and RdRp (6M71) were obtained from RCSB protein data bank (PDB). Water molecules, ligand molecules, if any present were removed from the structures prior to docking. Since, there has been no structural model available for Epro and MGpro, we have generated homology models from the protein sequences (YP_009724392.1 and YP_009724393.1) using SWISS-MODEL web server (Water house *et al.*, 2018) and evaluated their structural reliability before the virtual screening. SARS-CoV-2 envelope protein was taken as a template to build the model for Epro as SARS-CoV-2 shares high homology with SARS CoV (Gralinski *et al.*, 2020). Since MGpro shares homology to bidirectional sugar transporter SWEET2b, it was used as a template for building MGpro (Thomas, 2020) 3D structure. The structural validation of the 3D model was carried out using Rampage Ramachandran Plot Assessment web server (Tetko *et al.*, 2005).

2.2 Retrieval of *A. paniculata* active compounds

The flavones, sterols, and diterpene compounds from *A. paniculata* which have shown various medicinal properties were listed out by literature search. Further, they were screened *in silico* for their potential inhibition at the above-said target proteins. The structures of these compounds were obtained from PubChem. 7-O-methylwogonin (PubChem CID-188316), apigenin (5280443), onysilin (12041831), 3,4-dicaffeoylquinic acid (5281780), andrographolide (5318517), 14-deoxy-11,12-dihydroandro grapholide (5708351), neoandrographolide (9848024), 14-deoxyand rographolide (11624161), andrograponin (11666871), isoandrogra pholide (49841562), 3,19-isopropylidene andrographolide (16122395), 5-hydroxy 7,8-dimethoxyflavone (188316), β-sitosterol (222284), ergo sterol peroxide (5351516), 14-deoxy 14,15-dehydroandrographolide (6273762), 19-O-acetyl 14-deoxy 11,12-didehydroandrographolide (46179874), andrographolactone (44206466) and andrographic acid (16215024) were used in the present work. Nelfinavir (64143) and hydroxychloroquine (3652) were taken as reference molecules. All the ligand molecules downloaded in SDF format and prepared using the Marvin tools prior to docking.

2.3 Molecular virtual docking of various active compounds of *A. paniculata* at different SARS-CoV-2 targets

In silico, molecular docking studies were carried out using Molegro Virtual Docker. The processed ligand molecules and target receptors were docked by setting up gird center and grid size with energy minimization by running 1500 iterations for each run. Grid center was set around the active sites of each target and a separate run was performed for each target. The output poses/conformers that have been obtained after each docking were categorized based on the MolDock scores by the algorithm. The number of hydrogen bond interactions between the active site and ligand molecules was calculated.

2.4 Estimation of biological activity, pharmacological behavior, drug-likeness and toxicity for *A. paniculata* active metabolites

In addition to the docking, the bioavailability of all the secondary metabolites used in the present study was carried out. Using an ALOGPS 2.1 web server (Lipinski. 2004) lipophilicity (log P) and aqueous solubility (log S) were estimated based on the electro-topological state indices and associative neural network modeling. The log P and log S are the two crucial parameters for quantitative structure-property relationship (QSPR) studies. Compounds were submitted in SDF format to the ALOGPS 2.1 non-java interface for calculation of log p and log S values. The prediction of drug-like and non-drug like candidates was carried out using the Lipinski Rule of Five (Banerjee *et al.*, 2018). Prediction of toxicities for the active molecules that show the best inhibitory properties on various SARS-CoV-2 receptors was calculated using the Pro Tox-II web server (Masters, 2006). The toxicity of the molecules was represented in LD50 values (mg per kg body weight). Compounds were submitted to the server in SMILES format.

3. Results

3.1 Structure validation of 3D models generated for MGpro and Epro receptors of SARS CoV-2

The structure validation of MGpro and Epro receptor molecules by RAMPAGE analysis revealed the structural reliability of the modeled 3D structures. In the Ramachandran plot, most of the amino acid residues observed to be presented in the favored regions of the plot. The 98% of the amino acids were observed to be present in the most favored regions of the MGpro 3D model, and 2% of the amino acids were observed to be present in the allowed regions of the plot none of the amino acids were present in the outlier region of the plot. In the case of Epro, 92.9% of the amino acid residues were observed in the favored region, 3.9% were present in the allowed region and only 9 amino acids were observed in the outlier region of the plot.

3.2 Computational docking studies

The binding energies (MolDock scores) obtained from docking studies are an indicator of ligand-receptor complex formation. The higher negative MolDock score suggests a more favorable binding mode between the ligand and receptor with a better fit. The binding energies were compared to the reference molecule's binding energies (NFR and HCQ). NFR binding energies were observed to be higher than HCQ at different targets. The MolDock scores of all the compounds were given in Table 1.

The bioactive compounds such as 3,4-dicaffeoylquinic acid, neoandrographolide and isoandrographolide were observed to be top three ligands showing high binding energies than the reference drugs at almost all targets. Other compounds showing high binding energies than the reference drugs HCQ and NFR were given in the Table 1 along with their MolDock scores.

At the SGpro target (6VSB), the amino acids Arg (at 346, 355, 509 positions), Trp (436), Ser (373, 375, 438), Gly (496), Ile (418), Lys (417), Thr (345, 415), Asn (354, 437, 440), Asp (442), Leu (441), Gln (409), Glu (340), Tyr (453, 505) and Val (344) observed to be interacting partners in the hydrogen bond (HB) formation between target and ligand molecules (Figure 2) where as the Tyr (46, 69, 71), Arg (48, 49, 67, 109), Thr (9, 51, 75), Asn (7, 8), Asp (88), Leu (5), Lys (87), Glu (78) and Ala (79) are the interacting partners at Npro (6YI3) target (Figure 3).

Table 1: Receptor inhibitory efficiencies of bioactive compounds from *A. paniculata* plant at various receptors of SARS-CoV-2 virus. Inhibition efficiencies were represented in MolDock scores using Molegro Virtual Docker. Lesser the value higher the binding towards the receptor, hence higher the inhibition

SGpro (6VSB)	Npro (6YI3)	MGpro	3CLpro (6LU7)	PLpro (6W9C)	Nsp9 (6W4B)	Nsp15 (6VWW)	RdRp (6M71)	Epro
3,4- dicaffeoy-lquinic acid (-131.686)	3,4- dicaffeoy-quinic acid (-147.718)	3,4- dicaffeoy-quinic acid (-105.742)	3,4- dicaffeoy-quinic acid (-169.65)	3,4- dicaffeoy-quinic acid (-169.449)	3,4- dicaffeoy-quinic acid (-155.791)	3,4- dicaffeoy-quinic acid (-175.513)	Isoandrogra-pholide (-156.86)	3,4- dicaffeoy-quinic acid (-155.706)
Neoandrograp-holide (-118.181)	Nelfinavir (-133.822)	Nelfinavir (-96.610)	Nelfinavir (-165.7)	Isoandrograp-holide (-148.666)	Neoandrograp-holide (-137.572)	Neoandrograp-holide (-158.452)	3,4-dicaffeoyl-quinic acid (-150.123)	Isoandrogra-pholide (-129.260)
Isoandrogra-pholide (-116.946)	Neoandrograp-holide (-131.278)	Andrographo-lactone (-89.850)	Neoandrograp-holide (-149.41)	Neoandrograp-holide (-141.940)	Isoandrograp-holide (-137.387)	Nelfinavir (-145.663)	Nelifinavir (-149.479)	Nelfinavir (-128.736)
19-o-acetyl-14-deoxy 11,12-didehydro andrographolide (-109.068)	Isoandrograp-holide (-129.766)	Isoandrograp-holide (-83.355)	Isoandrograp-holide (-148.349)	Nelfinavir (-140.903)	Nelifinavir (-133.978)	ß-Sitosterol (-143.162)	Neoandrograp-holide (-130.312)	Neoandrograp-holide (-121.731)
Nelfinavir (-99.652)	19-o-acetyl-14-deoxy-11, 12-didehydro and-rographolide (-107.768)	19-o-acetyl-14-deoxy-11, 12-didehydro and-rographolide (-81.119)	ß-Sitosterol (-133.409)	ß- Sitosterol (-125.916)	ß- sitosterol (-108.635)	Isoandrograp-holide (-140.512)	19-o-acetyl-14-deoxy-11, 12-didehydro and-rographolide (-122.342)	19-o-acetyl-14-deoxy-11, 12-didehydro and-rographolide (-116.395)
ß-sitosterol (-99.440)	ß- sitosterol (-105.783)	Neoandrograp-holide (-81.096)	3,19-isopropy-lidene and-rographolide (-130.48)	Ergosterol peroxide (-124.793)	19-o-acetyl-14-deoxy-11, 12-didehydro and-rographolide (-107.212)	Andrographo-lactone (-126.238)	ß- sitosterol (-119.653)	ß - sitosterol (-103.882)
Andrograponin (-97.649)	3,19-isopropy-lidene androgr-apholide (-102.362)	ß- sitosterol (-80.755)	Andrographolac-tone (-127.89)	3,19-isopropy-lidene and-rographolide (-118.220)	3,19-isopropy-lidene and-rographolide (-104.609)	Andrographolide (-121.725)	3,19-isopropy-lidene and-rographolide (-118.935)	Hydroxychloro-quine (-103.398)
Andrographo-lactone (-93.011)	Androgra-pholide (-99.409)	Andrographic acid (-78.741)	Andrographolide (-125.849)	14-deoxy-11, 12-diheydro andrographolide (-116.068)	Andrographo-lactone (-104.559)	14-deoxy-14, 15-diheydro andrographolide (-121.607)	14-deoxy-14, 15-diheydro andrographolide (-115.204)	
3,19-isopropy-lidene andro-grapholide (-91.975)	14-deoxy-14,15 dehydro and-rographolide (-93.681)	3,19-isopropy lidene andro-grapholide (-77.186)	14-deoxy-11,12-diheydro andro-grapholide (-124.719)	19-o-acetyl-14, 15, dehydro andrographolide (-115.296)	Ergosterol peroxide (-102.28)	14-deoxy andro-grapholide (-118.738)	Andrographic acid (-112.892)	
14-deoxy and-rographolide (-89.169)	14-deoxy and-rographolide (-93.486)	14-deoxy and-rographolide (-72.019)	14-deoxy and-rographolide (-124.201)	Andrographic acid (-112.992)	Andrograp-holide (-99.366)	14-deoxy-11, 12-diheydro andrographolide (-117.478)	Andrograponin (-112.604)	
14-deoxy-14, 15 dehydro andrographolide (-87.407)	Andrograponin (-90.660)	Hydroxychlo-roquine (-71.886)	Andrograponin (-123.46)	Andrographo-lactone (-110.488)	14-deoxy and-rographolide (-98.490)	3,19-isopropy-lidene and-rographolide (-117.458)	14-deoxy-11, 12-didehydro andrographolide (-107.62)	
Andrographo-lide (-86.939)	Androgrpho lactone (-90.158)		19-o-acetyl-14 -deoxy-11,12-dedehydro and-rographolide (-121.901)	14-deoxy-14,15 dehydroandrogra-pholide (-108.792)	Andrograponin (-98.440)	Andrographic acid (-115.474)	Hydroxychloro-quine (-106.955)	
Hydroxy-chloroquine (-86.794)	14-deoxy-11, 12-didehydro andrographolide (-90.099)		Hydroxy-chloroquine (-121.084)	14-deoxyandrog grapholide (-108.238)	14-deoxy-11, 12-didehydro andrographolide (-97.206)	Ergosterol peroxide (-114.598)		
	Ergosterol peroxide (-89.556)			Onysilin (-103.372)	14-deoxy-14, 15 dehydroand-rographolide (-96.512)	Andrograponin (-114.24)		

Hydroxy-chloroquine (-87.851)		Hydroxy-chloroquine (-102.925)	Andrographic acid (-94.836)	19-o-acetyl-14-deoxy-11,12-didehydro and-rographolide (-114.203)		
			Onysilin (-89.519)	Hydroxy-chloroquine (-113.058)		
			Hydroxy-chloroquine (-88.534)			

Table 2: Lipinski's and ALOGPS values for the compounds showing high binding energies in the docking. Molecules having mass less than 500 daltons, less than 5 hydrogen bond donors, less than 10 hydrogen bond acceptors, Molar Refractivity between 40-130, Log P value not more than 5 and Log S value not more than -5 can be ideal for drug designing

| Compound | Lipinskis Rule | | | | | ALOGPS | |
	Mass	Number of H-bond donars	Number of H-bond acceptors	Molaa refractivity	Lop P	Log P	Log S
3,4-dicaffeoylquinic acid	516	7	12	125.19	1.02	2.05	-3.62
Neoandrographolide	480	4	8	123.41	1.84	1.88	-3.37
Isoandrographolide	592	1	5	169.76	7.21	7.42	-6.79
ß- sitosterol	414	1	1	128.21	8.02	7.27	-7.35
Andrograponin	318	1	3	90.78	4.02	4.28	-4.52
Andrographolactone	296	0	2	89.86	4.45	4.80	-5.34
3,19-isopropylidene andrographolide	390	1	5	105.37	3.76	3.12	-5.01
14-deoxyandrographolide	334	2	4	92.170	2.99	2.71	-3.51
14-deoxy-14,15 dehydroandrographolide	332	2	4	91.82	3.11	3.20	-3.70
Andrographic acid	364	4	6	96.38	2.38	3.12	-5.01
Hydroxychloroquine	335	2	4	98.27	3.78	3.87	-4.11
Nelfinavir	567	4	7	160.59	4.74	4.61	-5.47
19-o-acetyl-14-deoxy-11,12-didehydro andrographolide	374	1	5	101.62	3.33	3.57	-4.56
Onysilin	300	1	5	79.969	3.11	3.07	-3.69
14-deoxy-11,12-didehydro andrographolide	332	2	4	92.07	2.76	2.77	-3.61
Ergosterol peroxide	428	1	3	124.08	6.47	6.27	-7.33

The amino acids Thr (77), Ala (85), Cys (86), Val (88), Gly (89), Met (91), Trp (92), Ser (94), Phe (100) and Arg (101, 107) were involved in the binding of ligands to the active site of MGpro (Figure 4). At 3CLpro active site, the amino acids Glu (166), Cys (44, 145), His (41, 163, 164), Tyr (54), Asn (142), Leu (141), Ser (144), Phe (140), Asp (187), Thr (26, 190), Gln (143, 189, 192), Arg (188), Val (186) and Met (49) were observed as the interacting partners with ligand molecules (Figure 5).

The Thr (158, 301), Glu (161, 167), Asn (156, 267), Tyr (264, 268, 273), Asp (164), Lys (157) and Leu (162) were the active amino acid residues participating in the HB formations between active *A. paniculata* compounds and PLpro receptor (Figure 6), whereas amino acids such as Asp (26, 27), Ser (14, 60), Arg (40, 56), Thr (68), Pro (58), Val (42) and Gly (38) were the interacting partners at Nsp9 (6W4B) target site (Figure 7).

At Nsp15 (6VWW) target, the ligands were bound to target sites efficiently than HCQ (-115.009) with amino acids Thr (167), Lys (71, 90), Glu (203), Asn (200), Arg (199), Thr (196, 275), Lys (277), Val (295), Tyr (89, 279), Ser (198, 274), Glu (69), Asp (268, 273, 297), Gly (165) and Met (272) participating in the HB formation (Figure 8). The amino acids such as Tyr (32, 129, 619), Asn (138, 781), His (133), Lys (47, 714, 780), Asp (126, 135, 711, 761), Thr (141, 710), Leu (142), Ala (34, 130, 706, 762, 771), Ser (709, 772, 784), Gly (774), Gln (773) and Trp (617, 800) were identified as interacting partners of RdRp (6M71) active sites (Figure 9). At Epro Ala (22), Asn (64), Arg (61), Phe (20), Leu (28), Thr (30) and Val (25, 29) were the interacting partners of active sites involved in the HB formation (Figure 10).
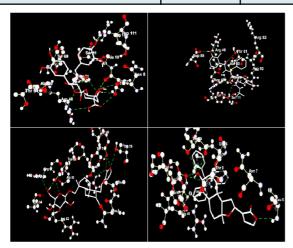
The binding energies and active amino acid molecules binding to different targets are given in Table 1. There are specific amino acids

identified as important in forming HB interactions. Arg, Ser and Asn at Spro; Arg, Tyr and Thr at Npro; His and Gln at 3CLpro; Tyr at PLpro; Pro, Asn, Ser, Arg at Nsp9; Thr, Lys at Nsp15; Ala and Asp at RdRp and Val at Epro targets were identified. The interactions between receptor and ligand were analyzed to find the hot spot amino acids involved in the interactions. We found that the hotspots residues Lys (90), Ser (274) at Nsp15 active site, Val (25, 29) at Epro, Pro (58) at Nsp9, Thr (301), Asp (164), Glu (167) at PLpro.

Table 3: Oral toxicity prediction results for the molecules of *A. paniculata* computed using Pro Tox -II web server

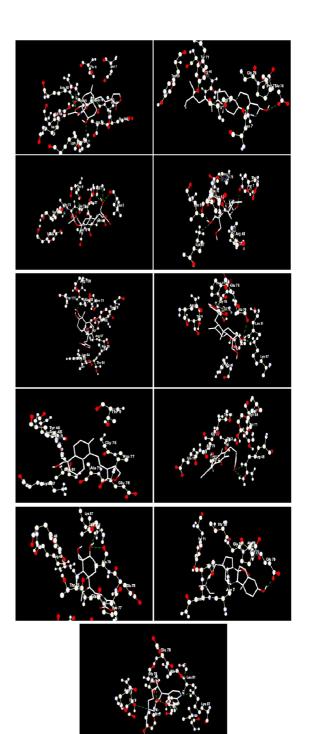| Compound	LD50 (mg per kg body weight)	Predicted toxicity class
14-deoxy-11,12-didehydro androgapholide	6060	6
3,4-dicaffeoylquinic acid	5000	5
Andrographic acid	3389	5
19-o-acetyl-14-deoxy-11,12-didehydro andrographolide	3389	5
Andrographolide	5000	5
Ergo sterol peroxide	2340	5
Isoandragrapholide	2000	4
ß- sitosterol	890	4
Andrographolactone	1400	4
3,19-isopropylidene andrographolide	1190	4
Onysilin	2000	4
Andrograponin	34	2
14-deoxyandrographolide	34	2
14-deoxy-14,15 dehydro andrographolide	34	2
Neoandrographolide	5	1
Hydroxychloroquine	1240	4
Nelfinavir	600	4

Figure 3: Docking conformers of active molecules present in *A. paniculata* at Npro (6YI3) receptor. (a) 3,4-dicaffeoylquinic acid, (b) nelfinavir, (c) neoandrographolide, (d) Isoandrographolide, (e) 19-o-acetyl-14-deoxy-11,12-didehydro andrographolide, (f) beta sitosterol, (g) 3,19-isopropylidene andrographolide, (h) andrographolide, (i) 14-deoxy-14,15 dehydro andrographolide, (j) 14-deoxyandrographolide, (k) andrograpanin, (l) andrographolactone, (m) 14-deoxy-11,12-didehydro andrographolide, (n) ergosterol peroxide, (o) hydroxychloroquine.
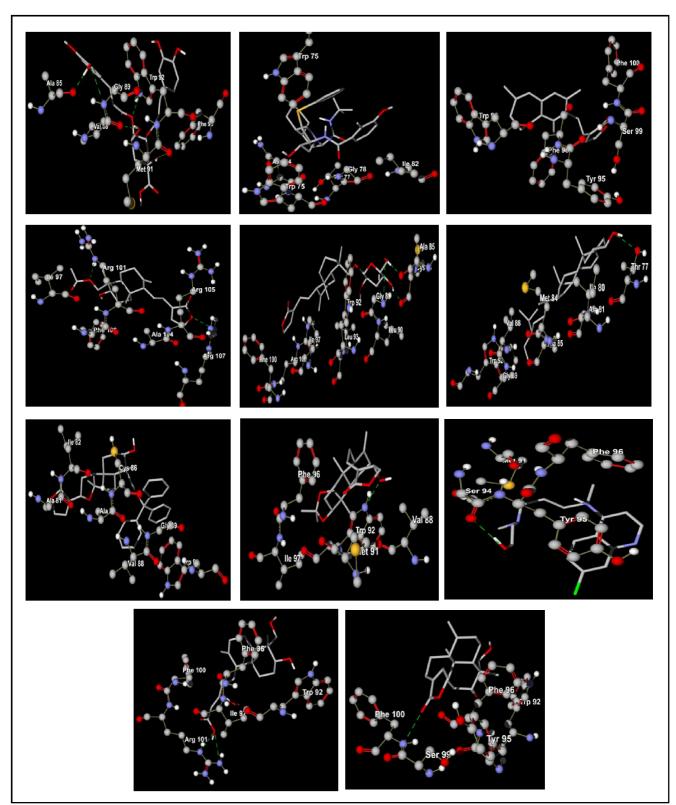
Figure 4: Docking conformers of active molecules present in *A. paniculata* at MGpro receptor. (a) 3,4-dicaffeoylquinic acid, (b) nelfinavir, (c) andrographolactone, (d) isoandrographolide, (e) 19-o-acetyl-14-deoxy-11,12-didehydro andrographolide, (f) neoandrographolide, (g) β-sitosterol, (h) andrographic acid, (i) 3,19-isopropylidene andrographolide, (j) 14-deoxyandrographolide and (k) hydroxychloroquine.
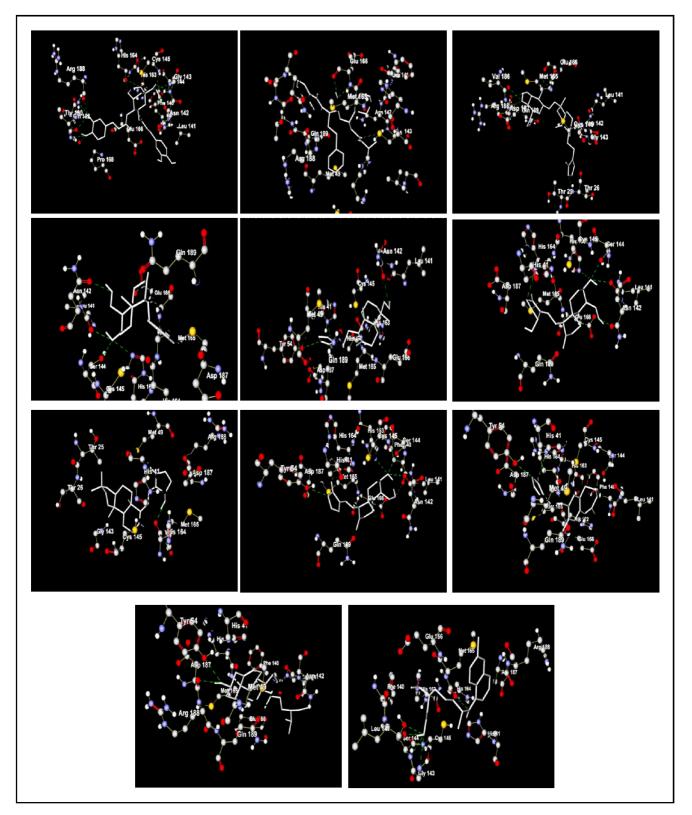
Figure 5: Docking conformers of active molecules present in *A. paniculata* at 3CLpro (6LU7) receptor. (a) 3,4-dicaffeoylquinic acid, (b) nelfinavir, (c) neoandrographolide, (d) 14-deoxyandrographolide, (e) andrograpanin, (f) andrographolide, (g) 3,19-isopropylidene andrographolide, (h) 14-deoxy-11,12-didehydroandrogapholide, (i) andrographolactone, (j) beta sitosterol, (k) hydroxychloroquine.
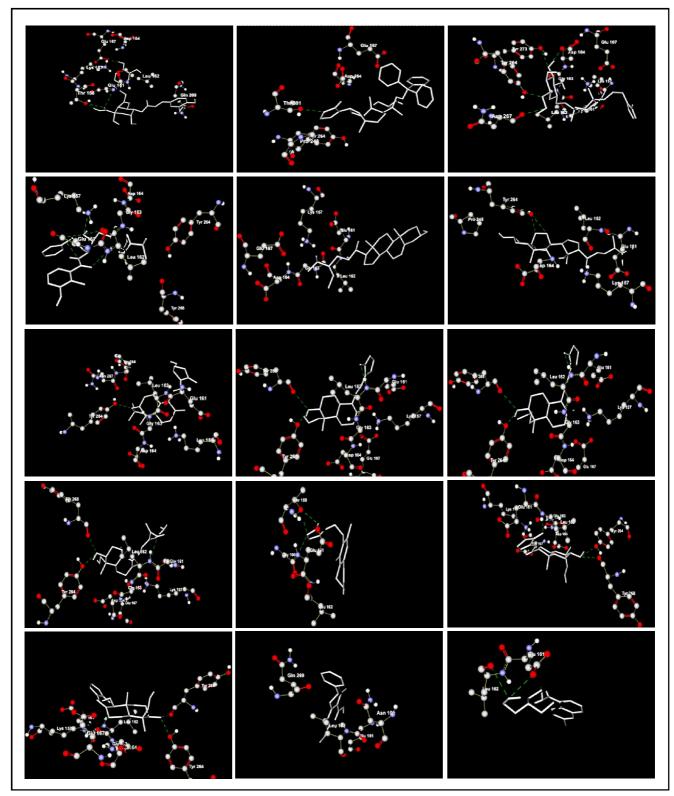
Figure 6: Docking conformers of active molecules present in *A. paniculata* at PLpro (6W9C) receptor. (a) 3,4-dicaffeoylquinic acid, (b) Isoandrographolide, (c) neoandrographolide, (d) nelfinavir, (e) beta sitosterol, (f) ergosterol peroxide, (g) 3,19-isopropylidene andrographolide, (h) 14-deoxy-11,12-diheydro andrographolide, (i) 19-o-acetyl-14,15,dehydro andrographolide, (j) andrographic acid, (k) andrographolactone, (l) 14-deoxy-14,15 dehydroandrographolide, (m) 14-deoxyandroggrapholide, (n) onysilin, (o) hydroxychloroquine.
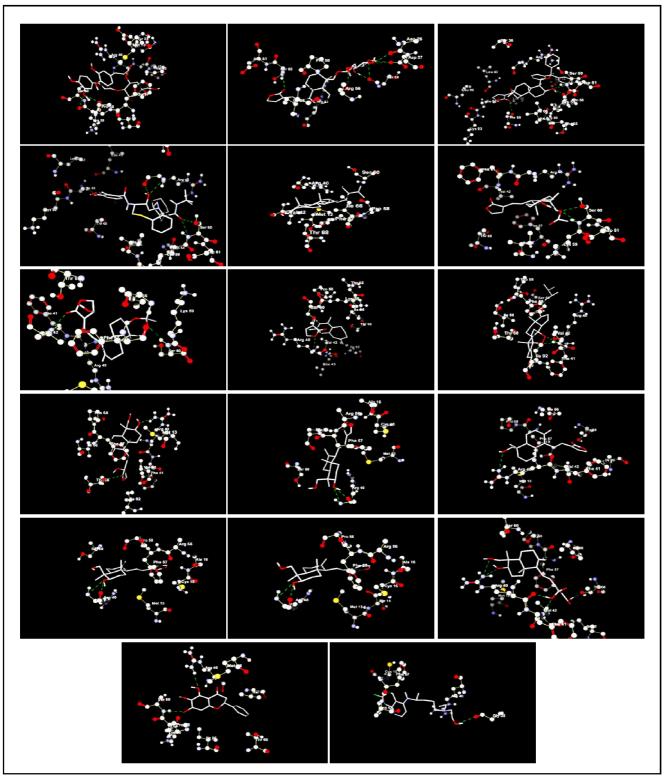
Figure 7: Docking conformers of active molecules present in *A. paniculata* at Nsp9 (6W4B) receptor. (a) 3,4-dicaffeonylquinic acid, (b) neoandrographolide, (c) Isoandrographolide, (d) nelifinavir, (e) beta sitosterol, (f) 19-o-acetyl-14-deoxy-11,12-didehydroandrographolide, (g) 3,19-isopropylidene andrographolide, (h) andrographolactone, (i) ergosterol peroxide, (j) andrographolide, (k) 14-deoxy andrographolide, (l) andrograpanin, (m) 14-deoxy-11,12-didehydroandrographolide, (n) 14-deoxy-14,15 dehydroandrographolide, (o) andrographic acid, (p) onysilin, (q) hydroxychloroquine.
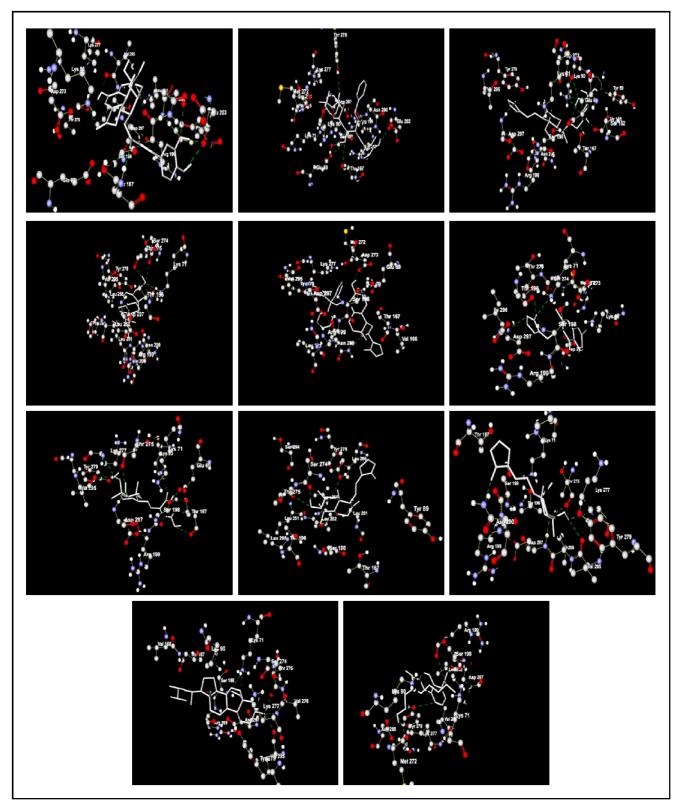
Figure 8: Docking conformers of active molecules present in *A. paniculata* at Nsp15 (6VWW) receptor. (a) 3,4-dicaffeonylquinic acid, (b) nelfinavir, (c) neo andrographolide, (d) beta-sitosterol, (e) iso andrographolide, (f) andrographolactone, (g) andrographic acid, (h) 19-o-acetyl-14-deoxy-11,12-didehydroandrographolide, (i) 14-deoxy-14,15-dehydro andrograp-holide, (j) ergosterol peroxide, (k) hydroxychloroquine.
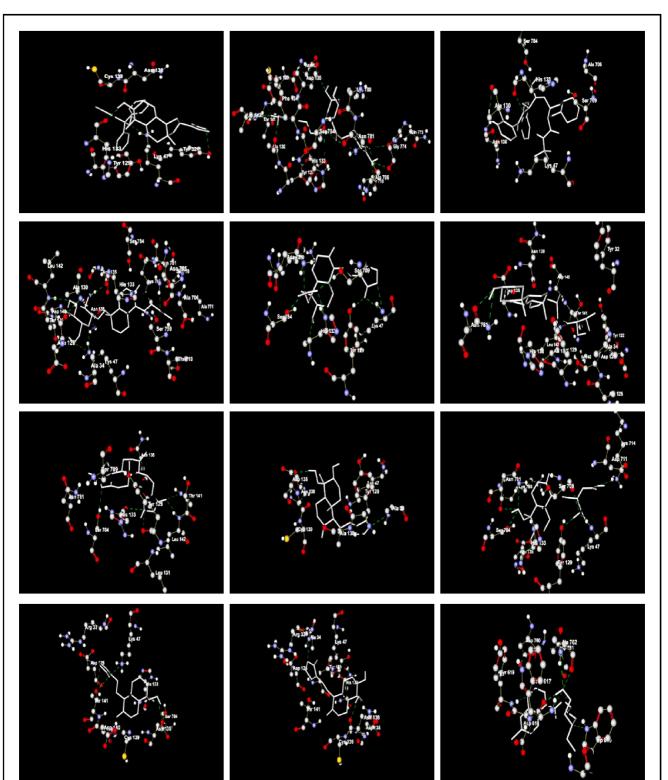
Figure 9: Docking conformers of active molecules present in *A. paniculata* at RdRp (6M71) receptor. (a) Isoandrographolide, (b) 3,4-dicaffeoylquinic acid, (c) nelifinavir, (d) neoandrographolide, (e) 19-o-acetyl-14-deoxy-11,12 didehydroandrographolide, (f) beta sitosterol, (g) 3,19-isopropylidene andrographolide, (h) 14-deoxy-14,15-dehydroandrographolide, (i) andrographic acid, (j) andrograpanin, (k) 14-deoxy-11,12-didehydro andrographolide, (l) hydroxychloroquine.
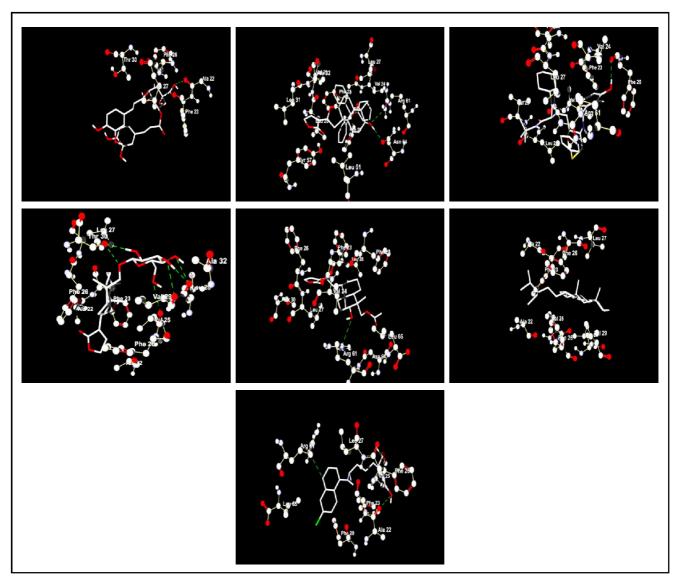
Figure 10: Docking conformers of active molecules present in *A. paniculata* at Epro receptor. (a) 3,4-dicaffeonylquinic acid, (b) iso andrographolide, (c) nelfinavir, (d) neo andrographolide, (e) 19-o-acetyl-14-deoxy-11,12-didehydroandrographolide, (f) beta-sitosterol, (g) hydroxychloroquine

3.3 Absorption, bioavailability, and drug-likeness of *A. paniculata* bioactive metabolites

The andrographolide, neoandrographolide, and andrographic acid have shown higher log P and log S values compared to other active compounds. Isoandrographolide which has shown higher binding affinities towards all the COVID-19 targets revealed high log P and least log S values. The log values of other *A. paniculata* active compounds were shown in Table 2.

The compounds that are following the Lipinski rule of 5 were listed in Table 2 along with ALOGPS values. All the compounds tested were observed to follow the 5 rules such as <5 hydrogen bond donors, <10 hydrogen bond acceptors, <500 daltons molecular mass, <5 log p and molecular refractivity in between 40-130. 3, 4-dicaffeoylquinic acid [(high molecular mass (592), molecular refractivity (169.76) and log P (7.21)] and isoandrographolide

[(more molecular mass (516), hydrogen bond donors (7) and acceptors (12)] slightly varied from the standard values.

3.4 Prediction of oral toxicity and LD50 values of active compounds from *A. paniculata*

The LD50 value is the lethal dose of a compound which required for killing 50% of test subjects upon exposure. The details of predicted LD50 values and class of toxicity of the active compounds from *A. paniculata* are shown in Table 3. The 14-deoxy 11, 12-didehydro andrographolide, 3, 4-dicaffeoylquinic acid, andrographic acid, 19-o-acetyl-14-deoxy 11, 12-didehydroandrographolide, andrographolide, ergo sterol peroxide, andrographolactone, 3, 19-isopropylidene andrographolide, onysilin have shown high LD50 values (800-6060 mg per kg body weight), whereas 14-deoxyandrographolide, 14-deoxy-14,15 dehydroandro-grapholide, andrograponin, and neoandrographolide were having less LD50 values (5-34 mg per kg body weight) and fall under class 1-2 of oral toxicity.

4. Discussion

The present study focused on multiple targets of SARS-CoV-2, involving essential structural and non-structural proteins. The inhibition of these targets can efficiently restrict the virus spread and subsequent disease treatment. The inhibitory mechanism of COVID-19 therapies involves the prevention of the virus entry into the host cell by acting on the host's specific receptors, preventing the synthesis and replication of viral RNA by interfering with functional proteins, thwarting the virus assembly, and inducing the host's innate immunity. In the present study, preventing the virus entry into the host cells by acting on the host's specific receptors such as MGpro, Epro, Npro, and SGpro was envisaged by *in silico* molecular docking approach. These are important host-specific proteins that play a crucial role in the entry of the virus into the host cells, hence inhibiting the SGpro, Epro, Npro, and MGpro is important and observed in the present study (McBride *et al.*, 2014). About half of the compounds used for *in silico* docking study were found to act on the targeted sites of these receptor molecules. The bioactive herbal compounds have shown low binding energies than the reference drugs, and thus exhibiting higher inhibition efficacy. The Npro plays an essential role in virus transcription and assembly by forming complexes with the viral RNA (Chang *et al.*, 2016). In a previous study conducted the Npro was considered as an important drug target against viruses (Jin *et al.*, 2020).

Preventing the virus RNA synthesis and replication can be achieved by acting on non-structural proteins which play a significant functional role involving RNA and protein synthesis (modification and processing). Amongst them, 3CLpro and PLpro are the important proteins due to their vital role in virus replication and subsequent host infection. The 3CLpro is essential for the virus maturation by proteolytic cleavage of the viral polyprotein (Khaerunnisa *et al.*, 2020). Inhibiting the action of 3CLpro can prevent the spread of the infection (Báez-Santos *et al.*, 2015; Mishra *et al.*, 2020). In the earlier study, it was revealed that the targeting of PLpro has an additional advantage over other targets as it acts like a two-sided sword and involved in viral replication and disrupting the signal cascade of apoptosis in uninfected cells surrounding the virus-infected cells (Egloff *et al.*, 2004). As evident from our docking results, most of the compounds were found effective in inhibiting the 3CLpro and PLpro, using the *A. paniculata* bioactive molecules offering additional advantages over other modern drug prescriptions.

Virus assembly can be prevented by blocking the non-structural proteins such as RNA binding protein (Nsp9), RNA dependent RNA polymerase (RdRp/Nsp12), and Nsp15 which play an important role in the replication-transcription complex (RTC). The inhibition of the RTC can be an efficient strategy in controlling COVID-19. Most of the phytochemicals from *A. paniculata* have shown inhibiting properties. Nsp9 protein binds to the ssRNA during replication/transcription and protects the newly synthesized RNA from nucleases (TeVelthuis *et al.*, 2010). Among the 15 non-structural proteins, Nsp12 was considered as the main RdRp for the RNA synthesis (Deng *et al.*, 2017). As Nsp15 plays a critical role in avoiding host immunity barriers, modulating its activity may possibly be used for developing live-attenuated vaccines (Efferth T and Koch. 2011).

The binding of active compounds to more than one target at the same time could enhance the therapeutic efficacy and decrease the chances of the development of drug resistance against single-target drugs. Especially, plant-based natural compounds are known to act against multiple targets (Sharma *et al.*, 2020). The validity of our results is supported by many recent studies where plant-based medicinal compounds were evaluated against COVID-19 virus such as non-structural proteins (Adem *et al.*, 2020), 3CLpro (Chandel *et al.*, 2020; Khalifa *et al.*, 2020; Bouchentouf and Missoum, 2020; Sharma and Kaur, 2020a, 2020b; Srivastava *et al.*, 2020; Bag and Bag, 2020), RdRp (Goswami *et al.*, 2020; Varshney *et al.*, 2020), SGpro (Bhowmik *et al.*, 2020; Subhash *et al.*, 2020; Wang *et al.*, 2020), 3CLpro and PLpro (Wu *et al.*, 2020). The compounds having higher or equal to the cutoff binding energies will be considered as candidate compounds for COVID-19 treatment. In the present study, the active compounds from the *A. paniculata* plant has shown high inhibition efficiencies towards multiple targets of the SARS-CoV-2 virus.

Moreover, *A. paniculata* plant used for centuries to treat many infectious diseases and considered as effective herbal preparation in arresting the spread of the influenza virus during the 1919 global flu epidemic. In recent days, *A. paniculata* concoction along with other medicinal plants was used as an immune booster in Indian (Ayurveda) and other traditional medicines such as 'Kan Jang' (Swedish Herbal Institute, N.H, USA), 'andrographis plus' (Metagenics Inc. CA, USA), 'stimuliv' (Franco-Indian Pharmaceutical Pvt. Ltd, Mumbai, India) and 'tribulus complex' (Jarrow Formulas, LA, USA). The enhancement of immunity in the individuals played a potential role in treating SARS patients in the recent past (Wang *et al.*, 2020). The compounds having anti-inflammatory properties exhibited immune-boosting agents in SARS patients and effectively controlled its spread (Kumar *et al.*, 2013). In addition to its anti-inflammatory properties and immune-boosting properties, most of the active metabolites were observed to interact efficiently with the SARS-CoV-2 targets as revealed from our *in silico* docking results. The combination of the docking result with support background literature, *A. paniculata* could be considered as an alternative plant-based lead drug formulation in the COVID-19 disease treatment and management.

The evaluation of log P and log S values are needed to compare their biological activity and pharmacological behavior inside the body. The compounds with high log P (more than 5) and low log S are considered as less absorbent and less soluble, respectively. The combined log P and log S values confirm their permeability of the compounds across cell membranes. The higher log P, lesser log S values implies poor absorption, poor solubility, and hence enhanced bioavailability (Tetko and Bruneau, 2004). Recent studies have proved that compounds having less log P values were given significant results in studies *in vivo*. Andrographolide, andrographic acid, neoandrographolide, 3,4-dicaffeoylquinic acid, 14-deoxyandrographolide, 14-deoxy 11,12-didehydroandrographolide, onysilin, 3,19-isopropylidene andrographolide, 14-deoxy, 14,15-dehydroandrographolide, 19-O-acetyl-14-deoxy 11,12-dide-hydroandrographolide, andrograponin and andrographolactone have the log P values in between 1.57-4.8, indicating their easy diffusion capability across the membranes. Their low log P values have shown their nature of permeability through lipid membranes. However,

isoandrographolide, ergosterol peroxide, and β-sitosterol have higher log P values in the range of 6.27-7.42. Though, isoandrographolide has higher inhibiting efficiencies on various COVID-19 targets, it has low permeability across the membranes. The lipophilicity influences ADMET (absorption, distribution, metabolism, excretion, and toxicity) properties along with toxicity (Ferreira and Andricopulo, 2019). The log S values of most of the compounds fall in between 3.09-4.56, indicating many of the compounds from *A. paniculata* are having good bioavailability. These compounds include andrographolide, neoandrographolide, andrographic acid, 14-deoxyandrographolide, 14-deoxy 11, 12-didehydroandrogra pholide, 3, 4-dicaffeoylquinic acid, onysilin, 14-deoxy 14, 15-dehydroandrographolide, 7-O-methylogonin, andrograponin and 19-O-acetyl-14-deoxy 11,12-didehydroandrographolide. Though, 3, 19-isopropylidene andrographolide, andrographolactone having good permeability (Their log P values are 3.12 and 4.8, respectively) their log S values (-5.01 and -5.34, respectively) shown their poor bioavailability. Solubility of isoandrographolide, ergosterol peroxide, and β-sitosterol were observed to be low because of their less log S values (-6.79, -7.33 and -7.35, respectively). These values are consistent with their log P values as low solubility implies less absorption and hence, bioavailability. In particular, the andrographolide, andrographic acid, neoandrographolide, 3, 4-dicaffeoylquinic acid, 14-deoxyandrographolide, 14-deoxy 11, 12-didehydroandrographolide, onysilin and 14-deoxy 14, 15-dehydroandrographolide found to be more potent inhibitor from *A. paniculata* against COVID-19 in terms of their high cell permeability and bioavailability.

All the compounds exhibiting high, inhibiting properties of the various COVID-19 targets were observed to follow Lipinski rule of 5 except 3, 4-dicaffeoylquinic acid, and isoandrographolide. Hence, most of these compounds could be potential lead drug molecules and can be used for drug designing against the COVID-19 virus. Computational toxicity estimations are not only fastening the drug designing process but also determine toxic doses in animals by reducing the time spent on animal experiments. The compounds, most fall under the classes 4-6 in the oral toxicity levels which indicated the use of *A. paniculata* herbal preparation may not affect the individuals. The predicted LD50 values and toxicity indices revealed that all the active compounds from *A. paniculata* were non-toxic and can be used in the COVID-19 disease treatment and management in the form of herbal medicine preparations.

5. Conclusion

Our findings through *in silico* molecular docking demonstrated that most of the active compounds of *A. paniculata* have high binding affinities towards SARS-CoV-2 receptors and proved as efficient inhibitors. Importantly, most of the compounds have shown a high affinity not only to one target protein but also to multiple receptors. The binding energies of all these compounds are found to be higher than those of HCQ, which is currently being used in the treatment of COVID-19 and antiviral drug NFR. Due to toxicity and side-effects of chemical drugs, the use of traditional Indian herbal medicine may be an alternative approach in the treatment and management of COVID-19. Since *A. paniculata* has credited as a wonder drug for arresting the spread of the influenza epidemic during 1919, our findings find its significance towards the use of the plant as an adjunct drug in the current COVID-19 pandemic. With its disease

suppressing abilities and receptor inhibition efficiencies *A. paniculata* herb could be developed as a traditional therapeutic formulation to fight against COVID-19 with fewer side effects as the vaccines are not effectively arresting the spread of the disease.. As almost all the compounds possess drug-likeness, they can be used in drug designing against the COVID-19 virus. Based on our present finding, we hypothesize that the *A. paniculata* plant may potentially attenuate and restrict the spread of the virus. However, *in vivo* experiments with all COVD-19 variants are necessary to validate for the use of biological active molecules from *A. paniculata* either for drug designing, disease treatment, and management.

Authors' contributions

Study design and conception: MDS, MS. Data collection: MDS, MS. Data analysis: MDS, MS, BCK. Drafting the manuscript: MDS, MS. Critical Review, Editing the manuscript and Supervision: CCG. All authors read and approved the final version of the manuscript.

Conflict of interest

The authors declare that there are no conflicts of interest relevant to this article.

References

Adem, S.; Eyupoglu, V.; Sarfraz, I.; Rasul, A. and Ali, M. (2020). Identification of potent COVID-19 main protease (Mpro) inhibitors from natural polyphenols: An *in silico* strategy unveils a hope against CORONA. Preprints, 2020;http://doi:10.20944/preprints202003.0333.v1.

Ali-Seyed, M. and Vijayaraghavan, K. (2020). Dengue virus infections and anti-dengue virus activities of *Andrographis paniculata*. Asian Pac. J. Trop. Med., 13(2):49.

Angamuthu, D.; Purushothaman, I.; Kothandan, S. and Swaminathan, R. (2019). Antiviral study on *Punica granatum* L., *Momordica charantia* L., *Andrographis paniculata* Nees, and *Melia azedarach* L., to human herpes virus-3. Eur. J. Integr. Med., 28:98-108.

Bag, A. and Bag, A. (2020). Treatment of COVID-19 patients: *Justicia adhatoda* leaves extract is a strong remedy for COVID-19 - Case report analysis and docking based study. Preprint, https://doi. org/ 10.26434/chemrxiv, 12038604, v1.

Balkrishna, A.; Pokhrel, S.; Singh, J. and Varshney, A. (2020). Withanone from *Withania somnifera* may inhibit novel coronavirus (COVID-19) entry by disrupting interactions between viral S-protein receptor binding domain and host ACE2 receptor. Research Square, 2020;http:// doi:10.21203/rs.3.rs-17806/v1.

Balasubramaniam, M. and Reis, R.J.S. (2020). Computational target-based drug repurposing of elbasvir, an antiviral drug predicted to bind multiple SARS-CoV-2 proteins. Chem. Rxiv., 10:1-20.

Báez-Santos, Y.M.; John, S.E.S. and Mesecar, A.D. (2015). The SARS-coronavirus papain-like protease: Structure, function and inhibition by designed antiviral compounds. Antiviral Res., 115:21-38.

Banerjee, P.; Eckert, A.O.; Schrey, A.K. and Preissner, R. (2018). ProTox-II: A webserver for the prediction of toxicity of chemicals. Nucleic Acids Res., 46(1):257-263.

Barros, R.O.; Junior, F.L.; Pereira, W.S.; Oliveira, N.M. and Ramos, R. M. (2020). Interaction of drug candidates with various SARS-CoV-2 receptors: An *in silico* study to combat COVID-19. J. Proteome Res., **19**(11):4567-4575.

Bhowmik, D.; Nandi, R.; Prakash, A. and Kumar, D. (2021). Evaluation of flavonoids as 2019-nCoV cell entry inhibitor through molecular docking and pharmacological analysis. Heliyon, **7**(3):e06515.

Bouchentouf, S. and Missoum, N. (2020). Identification of compounds from *Nigella sativa* as new potential inhibitors of 2019 novel coronasvirus (COVID-19): Molecular docking study. Chem. Rxiv., **20**:20.

Cascarina, S.M. and Ross, E.D. (2020). A proposed role for the SARS-CoV-2 nucleocapsid protein in the formation and regulation of biomolecular condensates. FASEB J., **34**(8):9832-9842.

Chang, C.K.; Lo, S.C.; Wang, Y.S. and Hou, M.H. (2016). Recent insights into the development of therapeutics against coronavirus diseases by targeting N protein. Drug Discov. Today, **21**(4):562-572.

Chen, N.; Zhou, M.; Dong, X.; Qu, J.; Gong, F.; Han, Y.; Qiu, Y.; Wang, J.; Liu, Y.; Wei, Y. and Yu, T. (2020). Epidemiological and clinical characteristics of 99 cases of 2019 novel coronavirus pneumonia in Wuhan, China: A descriptive study. Lancet, **395**(10223):507-513.

Churiyah, O.B. and Elrade, R. (2015). Antiviral and immunostimulant activities of *Andrographis paniculata*. HAYATI J. Biosci., **2**(22):67-72.

Colson, P.; Rolain, J. M.; Lagier, J.C.; Brouqui, P. and Raoult, D. (2020). Chloroquine and hydroxychloroquine as available weapons to fight COVID-19. Int. J. Antimicrob. Agents, **55**(4):105932.

Dai, Y.; Chen, S. R.; Chai, L.; Zhao, J.; Wang, Y. and Wang, Y. (2019). Overview of pharmacological activities of *Andrographis paniculata* and its major compound andrographolide. Crit. Rev. Food Sci., **59**(1):17-29.

Deng, X.; Hackbart, M.; Mettelman, R.C.; O'Brien, A.; Mielech, A.M.; Yi, G.; Kao, C.C. and Baker, S.C. (2017). Coronavirus nonstructural protein 15 mediates evasion of dsRNA sensors and limits apoptosis in macrophages. Proc. Natl. Acad. Sci. USA, **114**(21):E4251-E4260.

Egloff, M.P.; Ferron, F.; Campanacci, V.; Longhi, S.; Rancurel, C.; Dutartre, H.; Snijder, E.J.; Gorbalenya, A.E.; Cambillau, C. and Canard, B. (2004). The severe acute respiratory syndrome-coronavirus replicative protein nsp9 is a single-stranded RNA-binding subunit unique in the RNA virus world. Proc. Natl. Acad. Sci. USA, **101**(11):3792-3796.

Efferth, T. and Koch, E. (2011). Complex interactions between phytochemicals. The multi-target therapeutic concept of phytotherapy. Curr. Drug Targets, **12**(1):122-132.

Ferreira, L.L. and Andricopulo, A.D. (2019). ADMET modeling approaches in drug discovery. Drug Discov. Today, **24**(5):1157-1165.

García, C. C.; Sánchez, E. A.; Huerta, D. H. and Gómez-Arnau, J. (2020). Covid-19 treatment-induced neuropsychiatric adverse effects. Gen. Hosp. Psychiatry, **63**:163-164.

Gevers, S.; Kwa, M.S.G.; Wijnans, E. and Van Nieuwkoop, C. (2020). Safety considerations for chloroquine and hydroxychloroquine in the treatment of COVID-19. Clin. Microbiol. Infect., **26**(9):1276-1277.

Goswami, D.; Kumar, M.; Ghosh, S.K. and Das, A. (2020). Natural product compounds in alpinia officinarum and ginger are potent SARS-CoV-2 papain-like protease inhibitors. Chem. Rxiv. **10**:20-29.

Gralinski, L.E. and Menachery, V.D. (2020). Return of the coronavirus: 2019-nCoV. Viruses, **12**(2):135.

Hancke, J.; Burgos, R.; Caceres, D. and Wikman, G. (1995). A double blind study with a new monodrug Kan Jang: Decrease of symptoms and improvement in the recovery from common colds. Phytother Res., **9**(8):559-562.

Hsieh, Y.C.; Li, H.C.; Chen, S.C. and Lo, S.Y. (2008). Interactions between M protein and other structural proteins of severe, acute respiratory syndrome-associated coronavirus. J. Biomed. Sci., **15**(6):707-717.

Khaerunnisa, S.; Kurniawan, H.; Awaluddin, R.; Suhartati, S. and Soetjipto, S. (2020). Potential inhibitor of COVID-19 main protease (Mpro) from several medicinal plant compounds by molecular docking study. Preprints, http://doi:10.20944/preprints202003.0226.v1.

Khalifa, I.; Zhu, W.; Nafie, M.S.; Dutta, K. and Li, C. (2020). Anti-COVID-19 effects of ten structurally different hydrolysable tannins through binding with the catalytic-closed sites of COVID-19 main protease: An in-silico approach. Preprints, 2020;http://doi:10.20944/preprints 20 2003.0277.v1.

Kumar, D.; Chandel, V.; Raj, S. and Rathi, B. (2020). *In silico* identification of potent FDA approved drugs against coronavirus COVID-19 main protease: A drug repurposing approach. Chem. Biol. Lett., **7**(3):166-175.

Kumar, V.; Jung, Y.S. and Liang, P.H. (2013). Anti-SARS coronavirus agents: a patent review (2008-present). Expert. Opin. Ther. Pat. **23**(10): 1337-1348.

Jin, Z.; Du, X.; Xu, Y.; Deng, Y.; Liu, M.; Zhao, Y.; Zhang, B.; Li, X.; Zhang, L.; Peng, C. and Duan, Y. (2020). Structure of M pro from SARS-CoV-2 and discovery of its inhibitors. Nature, **582**(7811):289-293.

Li, F.; Lee, E. M.; Sun, X.; Wang, D.; Tang, H. and Zhou, G. C. (2020). Design, synthesis and discovery of andrographolide derivatives against Zika virus infection. Eur. J. Med. Chem., **187**:111925.

Li, S.Y.; Chen, C.; Zhang, H.Q.; Guo, H.Y.; Wang, H.; Wang, L.; Zhang, X.; Hua, S.N.; Yu, J.; Xiao, P.G. and Li, R.S. (2005). Identification of natural compounds with antiviral activities against SARS-associated coronavirus. Antiviral Res., **67**(1):18-23.

Lipinski, C.A. (2004). Lead-and drug-like compounds: the rule-of-five revolution. Drug Discov Today Technol., **1**(4):337-341.

Lu, H.; Stratton, C.W.; and Tang, Y.W. (2020). Outbreak of pneumonia of unknown etiology in Wuhan, China: The mystery and the miracle. J. Med. Virol., **92**(4):401-402.

Lu, R.; Zhao, X.; Li, J.; Niu, P.; Yang, B.; Wu, H.; Wang, W.; Song, H.; Huang, B.; Zhu, N. and Bi, Y. (2020). Genomic characterisation and epidemiology of 2019 novel coronavirus: Implications for virus origins and receptor binding. Lancet, **395**(10224):565-574.

Masters, P.S. (2006). The molecular biology of coronaviruses. Adv. Virus Res., **66**:193-292.

McBride, R.; Van Zyl, M. and Fielding, B.C. (2014). The coronavirus nucleocapsid is a multifunctional protein. Viruses, **6**(8):2991-3018.

Mishra, R.C.; Kumari, R.l Yadav, S. and Yadav, J.P. (2020). Antiviral potential of phytoligands against chymotrypsin-like protease of COVID-19 virus using molecular docking studies: An optimistic approach. Preprints, 2020;http://doi:10.21203/rs.3.rs-23956/v1.

Mitjà, O. and Clotet, B. (2020). Use of antiviral drugs to reduce COVID-19 transmission. Lancet Glob. Health, **8**(5):e639-e640.

Mousavizadeh, L. and Ghasemi, S. (2020). Genotype and phenotype of COVID-19: Their roles in pathogenesis. J. Microbiol. Immunol. Infect., **54**(2):159-163.

Mussard, E.; Cesaro, A.; Lespessailles, E.; Legrain, B.; Berteina-Raboin, S. and Toumi, H. (2019). Andrographolide, a natural antioxidant: An update. Antioxidants, **8**(12):571.

O'Donnell, V.B.; Thomas, D.; Stanton, R.; Maillard, J.Y.; Murphy, R.C.; Jones, S.A.; Humphreys, I.; Wakelam, M.J.; Fegan, C.; Wise, M.P. and Bosch, A., (2020). Potential role of oral rinses targeting the viral lipid envelope in SARS-CoV-2 infection. Function, **1**(1):p.zqaa002.

Paemanee, A.; Hitakarun, A.; Wintachai, P.; Roytrakul, S. and Smith, D.R. (2019). A proteomic analysis of the anti-dengue virus activity of andrographolide. Biomed. Pharmacother., **109**:322-332.

Pandey, P.; Rane, J.S.; Chatterjee, A.; Kumar, A.; Khan, R.; Prakash, A. and Ray, S. (2020). Targeting SARS-CoV-2 spike protein of COVID-19 with naturally occurring phytochemicals: An *in silico* study for drug development. J. Biomol. Struct. Dyn., pp:1-11.

Polash, S.A.; Saha, T.; Hossain, M.S. and Sarker, S. R. (2017). Investigation of the phytochemicals, antioxidant, and antimicrobial activity of the Andrographis paniculata leaf and stem extracts. Adv. Biosci. Biotechnol., **8**(05):149.

Puri, S.K.; Habbu, P.V.; Kulkarni, P.V. and Kulkarni, V.H. (2019). Characterization, *in vitro* antioxidant and hepatoprotective activity of fungal endophytic extracts of *Andrographis paniculata* leaves in CCL4 induced hepatotoxicity. Int. J. Pharm. Sci., **11**:44-54.

Sharma, A.; Tiwari, V. and Sowdhamini, R. (2020). Computational search for potential COVID-19 drugs from FDA-approved drugs and small molecules of natural origin identifies several antivirals and plant products. J. Bio. Sci., **45**(1):1-18.

Sharma, A. D. (2020). Eucalyptol (1, 8 cineole) from eucalyptus essential oil a potential inhibitor of COVID-19 coronavirus infection by molecular docking studies. http://doi:10.20944/preprints 202003 .0455.v1.

Sharma, A.D. and Kaur, I. (2020). Molecular docking studies on Jensenone from eucalyptus essential oil as a potential inhibitor of COVID-19 corona virus infection. arXiv preprint arXiv:2004.00217.

Srivastava, A.K.; Kumar, A. and Misra, N. (2020). On the Inhibition of COVID-19 Protease by Indian herbal plants: An *in silico* investigation. arXiv preprint arXiv:2004.03411.

Stubbs, T.M. and Te Velthuis, A.J. (2014). The RNA-dependent RNA polymerase of the influenza A virus. Future Virol., **9**(9):863-876.

Tallei, T.E.; Tumilaar, S.G.; Niode, N.J.; Kepel, B.J.; Idroes, R.; Effendi, Y.; Sakib, S.A. and Emran, T.B. (2020). Potential of plant bioactive compounds as SARS-CoV-2 main protease (Mpro) and spike (S) glycoprotein inhibitors: a molecular docking study. Scientifica, 2020. https://doi.org/10.1155/2020/6307457.

Te Velthuis, A.J.; Arnold, J.J.; Cameron, C.E.; Van den Worm, S.H. and Snijder, E.J. (2010). The RNA polymerase activity of SARS-coronavirus nsp12 is primer dependent. Nucleic Acids Res., **38**(1):203-214.

Tetko, I.V. and Bruneau, P. (2004). Application of ALOGPS to predict 1 octanol/water distribution coefficients, logP, and logD, of AstraZeneca in house database. J. Pharm. Sci., **93**(12):3103-3110.

Tetko, I.V.; Gasteiger, J.; Todeschini, R.; Mauri, A.; Livingstone, D.; Ertl, P.; Palyulin, V.A.; Radchenko, E.V.; Zefirov, N.S.; Makarenko, A.S. and Tanchuk, V.Y. (2005). Virtual computational chemistry laboratory-design and description. J. Comput. Aid. Mol. Des., **19**(6):453-463.

Thomas, S. (2020). The structure of the membrane protein of SARS-CoV-2 resembles the sugar transporter semi SWEET. Pathog. Immun., **5**(1):342.

Venkataraman, S.; Prasad, B.V. and Selvarajan, R. (2018). RNA dependent RNA polymerases: Insights from structure, function and evolution. Viruses, **10**(2):76.

Waterhouse, A.; Bertoni, M.; Bienert, S.; Studer, G.; Tauriello, G.; Gumienny, R.; Heer, F.T.; de Beer, T.A.P.; Rempfer, C.; Bordoli, L. and Lepore, R. (2018). SWISS-MODEL: Homology modelling of protein structures and complexes. Nucleic. Acids. Res., **46**(1):296-303.

Wang, L.S.; Wang, Y.R.; Ye, D.W. and Liu, Q.Q. (2020). A review of the 2019 Novel Coronavirus (COVID-19) based on current evidence. Inter. J. Antimicrob. Agents, **55**(6):1048-1059.

Wang, M.; Cao, R.; Zhang, L.; Yang, X.; Liu, J.; Xu, M.; Shi, Z.; Hu, Z.; Zhong, W. and Xiao, G. (2020). Remdesivir and chloroquine effectively inhibit the recently emerged novel coronavirus (2019-nCoV) *in vitro*. Cell Res., 30(3):269-271.

Weng, Z.; Chi, Y.; Xie, J.; Liu, X.; Hu, J.; Yang, F. and Li, L. (2018). Anti-inflammatory activity of dehydroandrographolide by TLR4/NF-κB signaling pathway inhibition in bile duct-ligated mice. Cellular Physiol. Biochem., **49**(3):1124-1137.

Wu, C.; Liu, Y.; Yang, Y.; Zhang, P.; Zhong, W.; Wang, Y.; Wang, Q.; Xu, Y.; Li, M.; Li, X. and Zheng, M. (2020). Analysis of therapeutic targets for SARS-CoV-2 and discovery of potential drugs by computational methods. Acta. Pharm. Sin. B., 10(5):766-788.

Xu, Z.; Peng, C.; Shi, Y.; Zhu, Z.; Mu, K.; Wang, X. and Zhu, W. (2020). Nelfinavir was predicted to be a potential inhibitor of 2019-nCov main protease by an integrative approach combining homology modelling, mole-cular docking and binding free energy calculation. Bio. Rxiv., **1201**:0-2.

Yen, C. C.; Chen, Y. C.; Wu, M. T.; Wang, C. C. and Wu, Y. T. (2018). Nanoemulsion as a strategy for improving the oral bioavailability and anti-inflammatory activity of andrographolide. Int. J. Nanomedicine, **13**:669.